eXPRESS Polymer Letters Vol.5, No.12 (2011) 1075–1084
Available online at www.expresspolymlett.com
DOI: 10.3144/expresspolymlett.2011.105

Permeability characterization of stitched carbon fiber preforms by fiber optic sensors

V. Antonucci[1*], *M. Esposito*[1], *M. R. Ricciardi*[1], *M. Raffone*[2], *M. Zarrelli*[1], *M. Giordano*[1]

[1]Institute for Composite and Biomedical Materials (IMCB-CNR), P.le E. Fermi, 1 80055, Portici (NA), Italy
[2]Alenia Aeronautica S.p.A., zona industriale ASI Incoronata, 71100 Foggia, Italy

Received 31 March 2011; accepted in revised form 26 June 2011

Abstract. The in-plane and through thickness permeability of unidirectional stitched carbon fiber preforms have been determined through vacuum infusion tests. The impregnation of various dry preforms with different stitching characteristics has been monitored by fiber optic sensors that have been stitched together with the dry tow to manufacture the dry preform. The experimental infusion times have been fitted by a numerical procedure based on Finite Element (FE) processing simulations. A good agreement between the numerical and experimental infusion times has been found demonstrating the potentiality of the fiber sensor system as suitable tool to evaluate impregnation times and permeability characteristics.

Keywords: *polymer composites, fiber optic sensor, permeability, VARTM*

1. Introduction

Liquid Composite Molding (LCM) processes have become increasingly popular for several industrial fields providing significant reduction of manufacturing costs compared with traditional autoclave processing and hand-lay up. Variations of this process include Resin Transfer Molding (RTM), vacuum-assisted RTM (VARTM), resin film infusion (RFI) and injection-compression RTM (I-CRTM). The common feature to all LCM processes is the impregnation of a dry fiber reinforcement by a thermoset liquid or film resin. The most popular technique is the RTM that consists in injecting a liquid resin in a closed mold containing the dry fiber preform. After the injection is completed, the mold is heated in order to activate the curing process.

Vacuum Assisted Resin Transfer Molding (VARTM) is a variant of the traditional resin transfer molding (RTM) process. VARTM process basically involves: lay up of a fiber preform, vacuum application, injection of a thermoset resin and resin cure. The reinforcement, typically carbon or glass fabric, is placed onto a one-sided rigid mold, on the other side a vacuum bag material replaces the common RTM matched metal tool. The resin is injected through one or more inlet gates, depending on part size and shape. Vacuum is applied through a single or multiple vents in order to remove the air from the fiber preform and to drive the fiber impregnation of the part by resin. A resin distribution medium is often placed onto the reinforcement to promote the resin flow, to eliminate voids and dry spots. This technology offers some advantages over the conventional RTM by saving the costs associated with matched-metal tooling, reducing volatiles emission and involving low injection pressures. Furthermore it provides better results than other production processes for the good repeatability and reliability of the material properties and enabling the production of cored structures in one operation. For these reasons VARTM is seeing increased commercial use for production of large quantities of parts.

*Corresponding author, e-mail: vinanton@unina.it

Currently, the VARTM process is commonly designed and optimized experimentally by trial-and-error approaches. This procedure requires a series of experiments in order to determine the optimal positioning of the resin injection gates and vacuum vents. To overcome critical manufacturing issues (dry zones) and optimize the process, some authors have developed numerical simulations able to model the resin infusion [1–9] during a VARTM process and active flow control methodologies to guarantee a filling uniformity [10, 11].

To predict the resin flow and model accurately the process, key input parameter is the permeability behaviour of the dry reinforcement preforms. Permeability measurements have been treated by numerous authors in the planar directions [12–16]. In addition, several studies deal with the subject of transverse permeability [18–21], that needs to be characterized especially in the case of processes like as VARTM process or the resin film infusion (RFI) [22]. In fact, conversely to RTM, these processes exhibit significant through-the-thickness impregnation gradients [23, 24] that may affect the total fiber impregnation, the filling time and, consequently, the dimensions and mechanical properties of the final composite part. In addition, due to the use of the flexible vacuum bag and, consequently, due to the variation of compaction pressure, the part thickness and local permeability of the fibre preform change during resin injection as function of time and space [25]. Therefore, to achieve a desired thickness in the final part, one should model the coupled fabric compaction and resin flow [26–28].

The most common technique to measure the permeability is to induce an unidirectional flow trough the reinforcement and monitor both the matrix front and the pressure as function of time [29]. Then, by the knowledge of the resin viscosity and total length to impregnate, the permeability is identified through the Darcy equation that relates linearly the resin velocity to the pressure gradient in the case of flow in porous media. This technique allows the permeability identification both in transient and saturated regime. However, the accuracy of the measurement can be compromised by 'race-tracking' effects. In fact, due to the larger flow along the mould edges, the permeability estimation could be greater than the real permeability of the preform. To overcome this issue, radial or three dimensional infusion experiments are performed for the in-plane or the three permeability components identification respectively. However, in the case of 3D infusion, complex three dimensional numerical simulations are generally required to evaluate the through thickness permeability. Therefore, due to the computation issues and the difficulty in following the flow front, unidirectional flow tests in saturated regime [30] are generally preferred to measure the through thickness permeability.

Alternatively, the use of discretely distributed sensors through the fiber reinforcement [31] can help the processing designer to determine the transient through thickness permeability. Ballata *et al*. [32] developed an electrical sensing grid for the *in-situ* flow monitoring during VARTM and determine the transverse transient permeability of glass random mats by a specific inverse method based on the mass conservation. Furthermore, Drapier *et al*. [30] designed a specific apparatus based on the use of optical-fibre sensors to detect the unidirectional resin flow trough a multiaxial fabric and identify the transient transverse permeability that resulted to be around a factor 10 larger than the saturated permeability.

In this study, the transient in-plane and through thickness permeability of eight stitched carbon fiber preforms have been identified during vacuum infusion tests using an aeronautical commercial epoxy resin. In particular, the resin advancement during the preform impregnation has been measured by using optical fibers that have been stitched preliminary together with the dry carbon tow during the preform manufacturing. In this way, the vacuum bag assembly procedures were simplified by limiting integration issues and the sensors position was fixed during the reinforcement impregnation. In addition, the in-plane and through thickness embedding of the optical sensors within the carbon preforms enabled to estimate the flow resistance of the preforms during a real vacuum infusion experiment by avoiding complex set-up. In fact, the permeability of the analysed fiber preforms has been identified by the best fitting of the experimental infusion times, evaluated by the sensor signals, and computation data, obtained by a three dimensional FE numerical processing simulation code.

2. Experimental

2.1. Preform characteristics

The in-plane and through thickness flow resistance of eight unidirectional stitched carbon fiber preforms (150 mm×150 mm) with different stitching characteristics has been investigated. In particular, two different carbon fibers (HTS 12k from Toho Tenax Europe GmbH, Heinsberg Germany, T800 12k from Toray Carbon fibers America, Flower Mound, USA) have been used to manufacture the fiber preforms that have been obtained by stitching eight unidirectional plies along the thickness direction. Each ply is made of dry carbon tows placed with the same orientation and stitched together by a zig-zag pattern with a stitching pitch of 5 mm for the lower and upper ply and a different stitching pitch for the other plies according with Table 1. Table 1 reports the characteristics of the stitched preforms in terms of fiber areal weight (FAW) and stitching pitch (SD) representing the superficial fiber density and the distance between two adjacent stitching points along the longitudinal direction of tow respectively (see Figure 1).

During the preform manufacturing, in accordance with the scheme shown in Figure 2, eight optical fibers were stitched in each fiber preform along the middle plane of the laminate and perpendicular to the carbon fibers. The sensors were used to monitor the resin advancement through the preform during the infusion. In addition, a reference optical fiber has been placed as very near as possible to the infusion tube in order to estimate the entry time of the resin as reference time for the eight sensor signals. Figure 3 shows a picture of a dry fiber preform with the optical fibers that exit from the reinforcement.

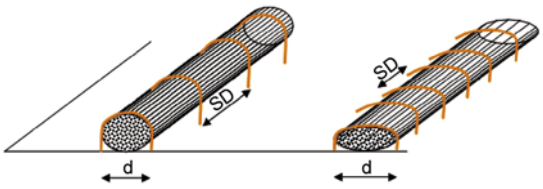

Figure 1. Stitching schematic

Table 1. Preforms stitching characteristics

Id. preformm	Carbon fiber	FAW [g/m^2]	Stitching pitch [mm]
1	HTS	270	5
2	HTS	270	30
3	HTS	270	50
4	HTS	340	5
5	HTS	400	5
6	T 800	230	5
7	T 800	230	30
8	T 800	230	50

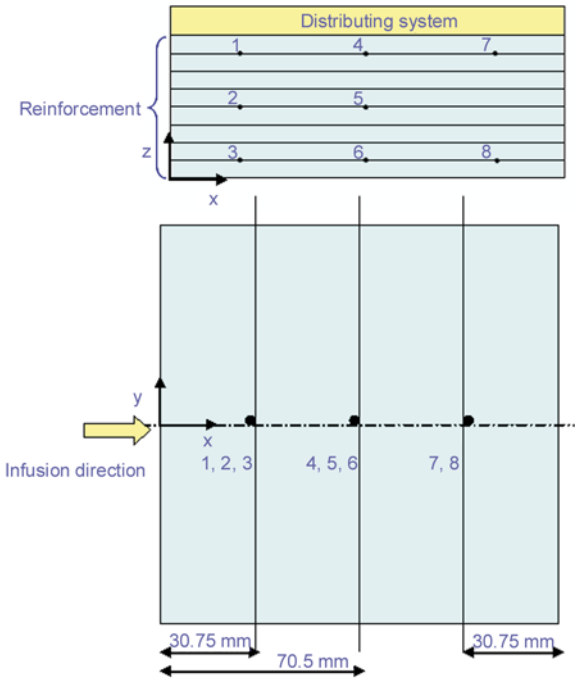

Figure 2. Schematic of optical fiber position

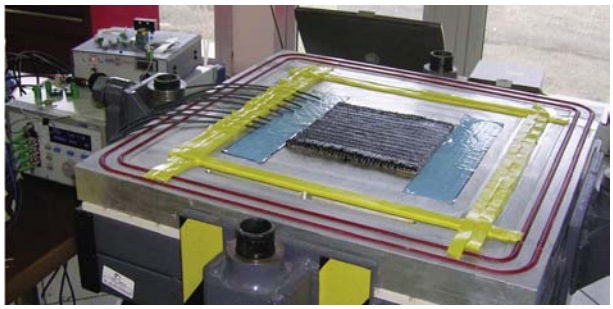

Figure 3. Dry perform with optical fibers

2.2. Sensor system

The fiber optic sensor is a powerful tool to perform remote, on-line, *in-situ* monitoring of composite manufacturing processes being free from electromagnetic interference and having high chemical and high temperature resistance. Furthermore, the fiber optical sensors can be multiplexed in several independent channels and embedded into the composite structure with minimally intrusive action due to the small size.

The hardware sensor apparatus consists of a personal computer, a data acquisition N.I. USB9215-A, an optical switch with eight channels (PRO800 from Thorlabs, Dachau, Germany), an home made

refractometer. This apparatus allows to monitor the reflectivity at the interface between the end of the optical fiber and the surrounding environment.
In particular, in this case, the resin flow front positions have been measured by using the fiber optic sensor based on the principle Fresnel reflection [32] and, thus, recording the refractive index. In fact, as a light beam is introduced into the fiber optic test segment, the optical signal is transmitted to the interface between the end of the optical fiber and the material, where the measurement is carried out. At the interface, part of the light beam is transmitted and part is reflected, depending on the refractive index mismatch between the fiber and the embedding material. The reflected signal is then back directed, by means of a fiber coupler to a photodetector. If a monomode fiber is employed, the intensity reflection coefficient R is given by Equation (1):

$$R = \left(\frac{n_f - n_m}{n_f + n_m}\right)^2 \quad (1)$$

where n_f and n_m are respectively the effective refractive index of the fiber and the sample refractive index.
The flow front position can be detected by recording the refractive index. In fact, as the optical fibers are embedded through the dry carbon reinforcement, a relatively large light signal is transmitted in absence of resin, in particular the 5% of the incident light is reflected back at the fiber-end/air interface. However, as the resin reaches the fiber/end interface, a significant dropping of the reflected signal is recorded. In this case, the mismatch between the refractive index of the resin and the fiber optical is very low being the refractive index of the epoxy resin (around 1.5) very close to the that one of the optical fiber. By placing several optical fibers in different locations, the resin advancement can be determined as it reaches each optical fiber.

2.3. Infusion tests

The composite panels have been manufactured by impregnating the carbon fiber preforms with the mono-component epoxy resin HexFlow® RTM 6 by Hexcel (Montluel, France). The infusion experiments have been designed to identify 3 orthogonal permeability components of eight unidirectional stitched preforms. The characteristics of the analysed performs are reported in Table 1. Therefore, to ensure the repeatability of the experimental measurements, 6 unidirectional preforms with the same stitching characteristics (Table 1) have been infiltrated: 3 of them have been impregnated by injecting the resin at 0° to measure the in-plane longitudinal permeability and 3 of them have been turned at 90° in order to inject the resin at 90° respect to the fiber reinforcement direction and measure the in-plane transverse permeability. In addition, the through thickness permeability has been identified by the measurement of the through thickness infiltration times and considering that the through thickness flow resistance of the 6 unidirectional preforms is the same.
The Vacuum Infusion process has been adopted according with the scheme of Figure 4, where it is possible to observe that three layers were stacked on the carbon reinforcement: the peel ply, the breather (Compoflex 150 of Fibertex Nonwovens, Aalborg, Denmark) and the flow distributing net (Green Flow – Airtech Europe Sarl, Differdange, Luxembourg) having different length to ensure different functions: the demolding, the vacuum distribution and the complete reinforcement wetting respectively. The resin injection and the vacuum were performed by two spiral pipes, connected respectively to the resin tank and to the vacuum pump. The whole system was sealed by the vacuum bag. A partial vacuum has been applied also to the resin container to reduce the local pressure variations and, hence, to minimize the thickness changes during the resin flow according with the study of Niggemann *et al*. [34] that have demonstrated the positive effect of this procedure for un-debulked preforms.
Figure 5 shows two pictures of the beginning and the end of the infusion tests.
In all tests, the resin injection temperature was settled at 80°C, while the mold temperature at 100°C. The vacuum pressure was set to 0.75 bar. Hence,

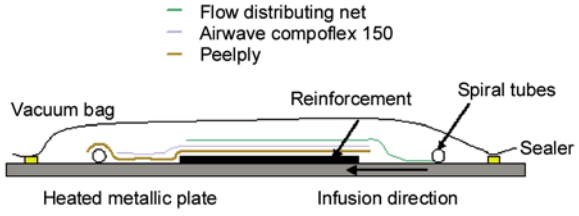

Figure 4. Schematic of infusion assembly system

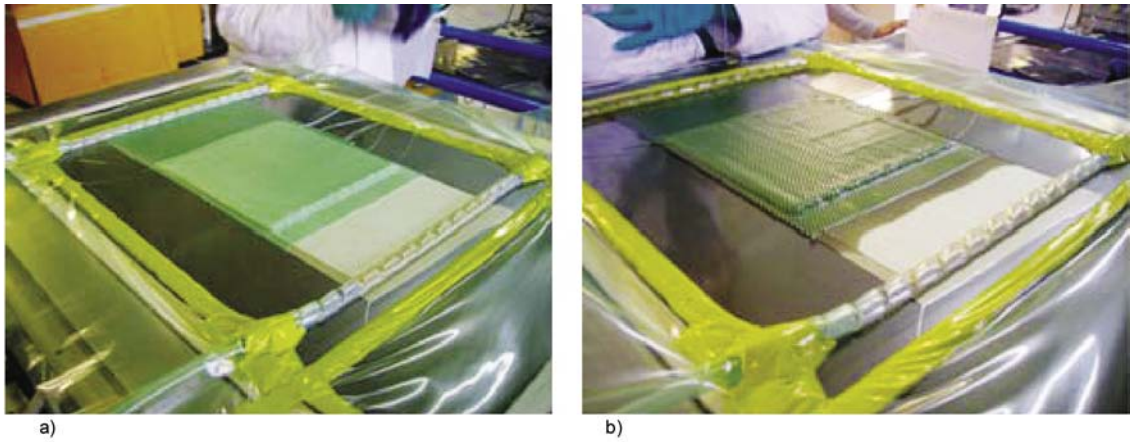

Figure 5. Beginning (a) and end of infusion (b) tests

Table 2. Composite characteristics

Id. preform	Average fibre volume fraction [%]	Average thickness [mm]
1	37.4	3.52±0,03
2	50.0	3.24±0.06
3	46.6	2.72±0.12
4	45.6	3.60±0.05
5	39.5	5.07±0,12
6	32.8	2.34±0.11
7	32.2	3.36±0.08
8	35.4	2.80±0.06

the experimental measurements and the permeability identification were performed just for the resulting unique fibre volume fraction. At the end of the fiber impregnation, the laminates have been consolidated by a cure cycle of 75 min at 160°C, followed by a plateau of 120 min at 180°C. The manufactured composite panels showed different characteristics in terms of final fiber volume fraction and thickness. Table 2 reports the averaged values of the fiber volume fraction and of thickness ± standard deviations for each perform.

3. FE processing simulation

The infusion process has been numerically simulated by the commercial finite element code PAM-RTM (ESI-GROUP, Italy) that adopts the Darcy law to describe the reinforcement impregnation [29, 31].

Since this software does not allow to create any type of geometry or mesh, the geometry and the mesh have been realized with an external code. Figure 6 shows the adopted FE model of the simulated test case. It should be noted that the model is two dimensional. In fact, just the cross section view of the distribution and reinforcement system has been considered for the numerical simulation. This assumption is based on the experimental observation that the resin generally exit from the infusion tube only after reaching the end of tube. Hence the resin flows simultaneously from all openings of the spiral infusion tube. This behaviour leads to an almost parallel resin front giving the possibility to neglect the influence of the flow along the direction parallel to the infusion tube.

Consequently, the elements for the FE model are two-dimensional (PLANE) and have a triangular shape (see Figure 6). The mesh size was selected with the objective to ensure an high level of accuracy for the individuation of the through-thickness permeability and considering that the thickness range was 3–5 mm. In particular, with reference to preform id. 5 a more refined mesh characterized by a lower longitudinal element size and aspect ratio about equal to one was also adopted finding filling times differences below 3%. According to Figure 6, the real experimental configuration of the vacuum bag assembly, consisting of the ancillary materials and dry preform, have been considered in the computational analysis. The different layers have been modelled and discretized. The first yellow layer

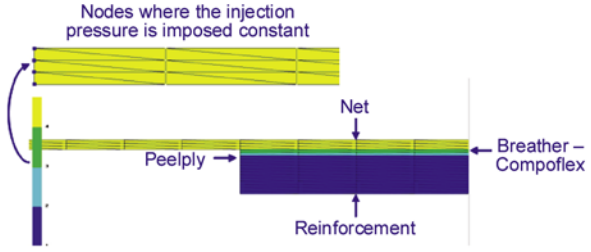

Figure 6. FE model: 1) reinforcement (blue); 2) peelply (cyan); 3) breather (green); 4) distributing net (yellow)

from the top is representative of the distribution network, then the green layer describes the breather material and, finally, the blue layer is for the peel ply. These layers are characterized by different permeability and length. In particular, the permeability characteristics have been determined preliminary by suitable experimental tests and assumed constant for all performed infusion tests. The values of the longitudinal/through thickness permeability of the different layers above the dry reinforcement were set to $2.05\cdot10^{-8}$ m^2/$2.537\cdot10^{-8}$ m^2, $2.042\cdot10^{-10}$ m^2/$1.6\cdot10^{-11}$ m^2, $1.62\cdot10^{-10}$ m^2/$3.5\cdot10^{-11}$ m^2, for distribution network, the breather and the peel ply respectively. Furthermore, it is possible to notice that the yellow top layer is longer than the others that have the same length of the fiber reinforcement. In fact, since the distributing net has the function to uniform and ease the resin flow, in the experimental tests it is placed close to the infusion tube and at a proper distance from the fiber reinforcement. This distance has been considered in the numerical simulations in order to take into account its influence on the pressure distribution and on the resin advancement. Otherwise, due to higher pressure gradients in the entry zone, the resin flow could result too fast and deviate from the real experimental data. Hence, the resin injection line has been fixed at the end of distribution net as shown in Figure 6, where the injection nodes are represented in blue. The injection pressure has been imposed constant and equal to 0.75 bar.

The resin flow has been considered isothermal. The resin viscosity and density have been assumed constant and equal to 0.7 Pa·s and 1140 kg/m^3 respectively.

4. Permeability data

The permeability values have been identified by the best fitting of the experimental impregnation times, defined as the time period needed to the resin front to reach the fiber optic sensor positions. As example, Table 3 shows the measured experimental times and the respective standard deviations for preform 5 for both infusion tests at 0 and 90° that resulted less than 20%. The sensor experimental measurements have been analysed by a proper developed numerical procedure that enables to run the commercial processing code PAMRTM in batch way. The processing simulations have been carried out simultaneously for the sixteen analysed infusion tests by changing the reinforcement permeability values and taking into account the different porosity and thickness values (Table 2) of final composites. In particular, it should be noticed that the fiber preform thickness and, hence, the permeability components for each preform have been assumed constant due to the observed low thickness gradient in the final composite (less than 1.5%).

Table 3. Experimental infusion times and the respective standard deviations for the preform 5

Sensor	0° infusion times [s]	90° infusion times [s]
1	5.91±1.18	9.52±0.09
2	9.27±2.39	9.85±1.21
3	9.78±3.33	11.43±0.09
4	17.57±2.39	18.18±1.27
5	19.62±2.15	19.33±1.33
6	19.49±2.41	20.34±0.85
7	25.22±3.33	26.33±1.33
8	29.09±4.98	28.68±0.15

After the evaluation of the numerical impregnation times, the Root Mean Square Error (RMSE) of the numerical results respect to the experimental sensor times have been evaluated as shown in Equation (2):

$$\mathrm{RMSE_{ik}} = \sqrt{\frac{\sum_{j=1}^{8}(t_{ijk} - T_{ij})^2}{8}} \tag{2}$$

where

– $\mathrm{RMSE_{ik}}$ is the error for the generic i test, with i ranging between 1 and 16 and k the permeability values assigned to the reinforcement for the i test;

– t_{ijk} is the numerical time that the resin employs to reach the j sensor (j ranges between 1 and 8, being 8 the number of the optical fibers) for the i test k the permeability values couple;

– T_{ij} is the objective experimental time that the resin employs to reach the j sensor (j ranges between 1 and 8) for the i test.

To establish the optimal permeability components, two concurrent criteria have been adopted:

– $\mathrm{RMSE_{ik}}$ has to be the minimum possible value;

– since the same reinforcement is impregnated with a 0 and 90° vacuum infusion test, its through thickness flow resistance and, consequently, the through thickness permeability has to be the same for both tests.

Table 4. Minimum error between experimental and numerical times

Id. preform	RMSE 0° infusion [s]	RMSE 90° infusion [s]
1	2.24	3.45
2	3.28	1.41
3	3.71	2.21
4	1.87	1.41
5	1.46	1.58
6	2.65	2.72
7	2.50	3.62
8	2.55	1.87

By the application of these criteria, the in-plane and through thickness permeability have been identified for each preform.

Tables 4 and 5 report the minimum RMSE and the corresponding identified permeability values for each test. As calculated, the RMSE values resulted less than 4 sec. In general, greater time differences have been found for the impregnation times relative to positions closer to the injection tube. As example, Figures 7a and 7b show the experimental and numerical infusion times for the preform '5', where it is possible to observe a good agreement between the two kinds of data. In addition, for this preform the effect of the standard deviations of the experimental times on the permeability values has been calculated. Starting from the average experimental time obtained for the i sensor, three levels of times have been considered: t_i–σ_{t_i} t_i, and t_i+σ_{t_i}, where σ_{t_i} is the standard deviation of the experimental times obtained for the *i* sensor, to evaluate the full factorial time table. Figures 8a–c report the resulting distribution of the permeability components K_x, K_y, K_z that show standard deviations equal to $4.57 \cdot 10^{-11}$, $2.77 \cdot 10^{-11}$, $7.792 \cdot 10^{-11}$ m^2 respectively.

From Table 5, it is possible to notice no large differences between the in-plane and the through thickness permeability components and a different dependence of the three permeability components on the preform stitching characteristics. In fact, the in plane permeability components don't show any dependence on FAW and SD being their values quite similar for the different preforms. This result come from the use of the distributing system that has low flow resistance and promote strongly the in-plane resin flow that so is uniformly distributed and is not affected by the in-plane flow resistance properties of the fiber reinforcement.

Otherwise, as expected, the through thickness permeability resulted lower than the in-plane permeability and is affected by the stitching characteristics. For similar FAW values, the through thickness permeability is an increasing function of the stitching pitch especially for SD variation from 5 to 30.

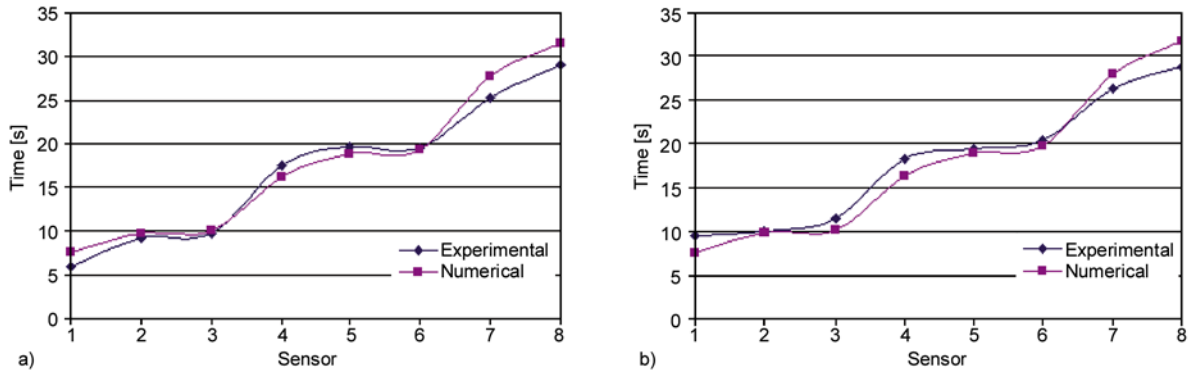

Figure 7. Experimental and numerical impregnation times for preform '5' a) 0° infusion; b) 90° infusion

Table 5. Permeability values

Id. preform	In plane longitudinal permeability [m^2]	In plane transverse permeability 90° fiber direction [m^2]	Through thickness permeability [m^2]
1	$5.93 \cdot 10^{-10}$	$1.66 \cdot 10^{-10}$	$0.75 \cdot 10^{-10}$
2	$9.42 \cdot 10^{-10}$	$8.25 \cdot 10^{-10}$	$4.40 \cdot 10^{-10}$
3	$8.25 \cdot 10^{-10}$	$6.70 \cdot 10^{-10}$	$5.00 \cdot 10^{-10}$
4	$9.61 \cdot 10^{-10}$	$4.95 \cdot 10^{-10}$	$2.35 \cdot 10^{-10}$
5	$8.64 \cdot 10^{-10}$	$7.67 \cdot 10^{-10}$	$4.80 \cdot 10^{-10}$
6	$3.99 \cdot 10^{-10}$	$2.83 \cdot 10^{-10}$	$0.95 \cdot 10^{-10}$
7	$10.0 \cdot 10^{-10}$	$0.69 \cdot 10^{-10}$	$3.00 \cdot 10^{-10}$
8	$9.42 \cdot 10^{-10}$	$9.03 \cdot 10^{-10}$	$4.20 \cdot 10^{-10}$

Furthermore, for the HTS based preforms, having the same SD (id. 1, 4, 5), the through thickness permeability depends powerfully on FAW.

In general, these results can be interpreted by considering that the permeability of stitched preforms is affected in a complex manner by the specific reinforcement architecture, microstructure and fibre areal weight. In particular, some literature papers [17, 22] have shown that the stitching enhances the flow resistance by providing additional flow paths for the resin. Drapier *et al*. [17] demonstrated that the through thickness permeability is not controlled by the stacking sequence and by the stitching patterns, but it seems to be determined by the stitching density.

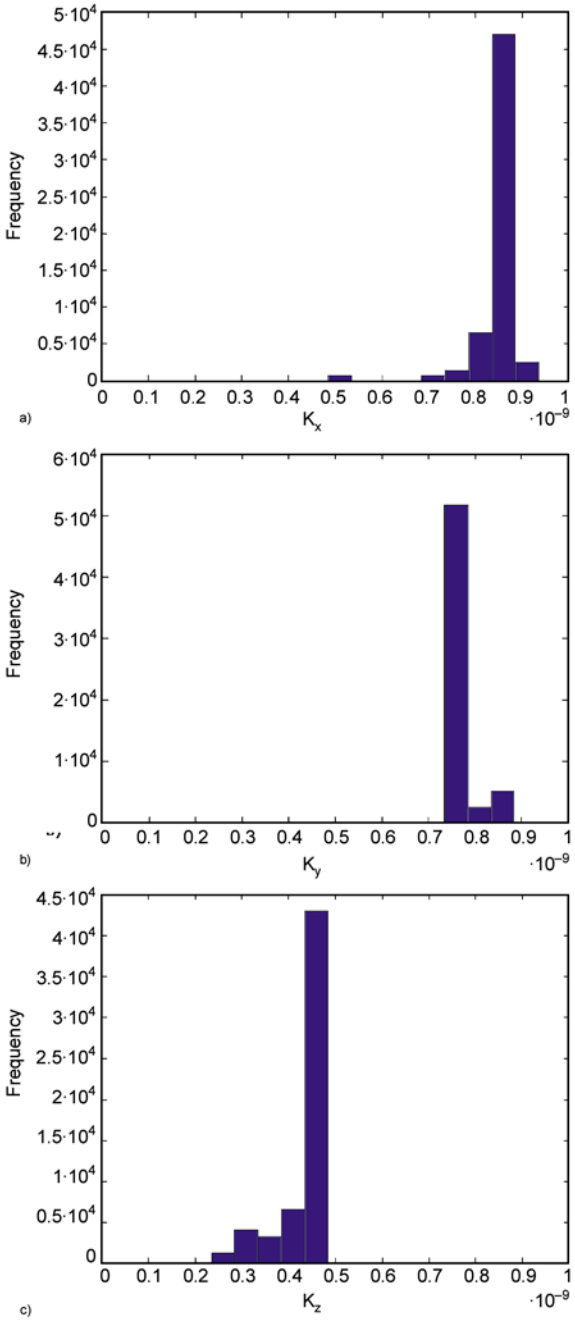

Figure 8. Permeability distributions for perform '5' a) In-plane longitudinal permeability K_x; b) In-plane transverse permeability K_y; c) Through thickness permeability K_z

The permeability results of this work seem to confirm that the investigated stitched preforms are characterized by low flow resistance and, hence, high permeability values along the three main directions. However, since it has been observed that the through thickness permeability is as increasing function of the stitching pitch parameter, it is possible to conclude that the though thickness flow resistance is influenced more by the void area left by adjacent stitching points than by the stitching density.

5. Conclusions

Vacuum infusion tests have been carried out to manufacture composite panel based on an aeronautical commercial resin and carbon fiber reinforcements. In particular, the carbon preforms have been realized by stitching, starting from two different carbon dry tows. In addition, in each investigated carbon preform eight optical fibers have been stitched along the middle plane of the lay-up in eight different positions in order to avoid undesired movements during the resin infusion. The optical fibers allowed to monitor the resin flow advancement during the vacuum infusion tests. The experimental impregnation times, obtained by the sensor signals, have been fitted by a numerical procedure based on the use of the commercial PAMRTM processing simulation code. In this way, the transient in-plane and through thickness permeability components have been identified for each fiber preform. The in-plane permeability resulted unaffected by the stitching characteristics of the preforms. On the other hand, the through thickness permeability has been found an increasing function of both the fiber areal weight and the stitching pitch of the preform. Thus, these results evidence that the distributing system has a great effect on the planar flow, having higher permeability than the reinforcement and the function to promote and homogenise the resin infiltration on the first laminate plies. Therefore, for the VARTM process and similar technologies the through-thickness permeability is the most important parameter to control the fiber impregnation and the processing time especially in the case of large

structures. Finally, the developed methodology can be a useful tool to measure the effective transient through thickness flow resistance of the reinforcements during the real process.

References

[1] Correia N. C., Robitaille F., Long A. C., Rudd C. D., Šimáček R. P., Advani S. G.: Use of resin transfer molding simulation to predict flow, saturation, and compaction in the VARTM process. Journal of Fluids Engineering, **126**, 210–215 (2004). DOI: 10.1115/1.1669032

[2] Hammami A., Gebart B. R.: Analysis of the vacuum infusion molding process. Polymer Composites, **21**, 28–40 (2000). DOI: 10.1002/pc.10162

[3] Kang M. K., Lee W. I., Hahn H. T.: Analysis of vacuum bag resin transfer molding process. Composites Part A: Applied Science and Manufacturing, **32**, 1553–1560 (2001). DOI: 10.1016/S1359-835X(01)00012-4

[4] Han K., Jiang S., Zhang C., Wang B.: Flow modeling and simulation of SCRIMP for composites manufacturing. Composites Part A: Applied Science and Manufacturing, **31**, 79–86 (2000). DOI: 10.1016/S1359-835X(99)00053-6

[5] Acheson J. A., Šimáček P., Advani S. G.: The implications of fiber compaction and saturation on fully coupled VARTM simulation. Composites Part A: Applied Science and Manufacturing, **35**, 159–169 (2004). DOI: 10.1016/j.compositesa.2003.02.001

[6] Šimáček P., Advani S. G.: Desirable features in mold filling simulations for liquid composite molding processes. Polymer Composites, **25**, 355–367 (2004). DOI: 10.1002/pc.20029

[7] Song Y. S., Youn J. R.: Modeling of resin infusion in vacuum assisted resin transfer molding. Polymer Composites, **29**, 390–395 (2008). DOI: 10.1002/pc.20326

[8] Hsiao K-T., Mathur R., Advani S. G., Gillespie J. W., Fink B. K.: A closed form solution for flow during the vacuum assisted resin transfer molding process. Journal of Manufacturing Science and Engineering, **122**, 463–476 (2000). DOI: 10.1115/1.1285907

[9] Li J., Zhang C., Liang R., Wang B., Walsh S.: Modeling and analysis of thickness gradient and variations in vacuum-assisted resin transfer molding process. Polymer Composites, **29**, 473–482 (2008). DOI: 10.1002/pc.20439

[10] Modi D., Correia N., Johnson M., Long A., Rudd C., Robitaille F.: Active control of the vacuum infusion process. Composites Part A: Applied Science and Manufacturing, **38**, 1271–1287 (2007). DOI: 10.1016/j.compositesa.2006.11.012

[11] Johnson R. J., Pitchumani R.: Simulation of active flow control based on localized preform heating in a VARTM process. Composites Part A: Applied Science and Manufacturing, **37**, 1815–1830 (2006). DOI: 10.1016/j.compositesa.2005.09.007

[12] Luce T. L., Advani S. G., Howard J. G., Parnas R. S.: Permeability characterization. Part 2: Flow behavior in multiple-layer preforms. Polymer Composites, **16**, 446–458 (1995). DOI: 10.1002/pc.750160603

[13] Lekakou C., Johari M. A. K., Norman D., Bader M. G.: Measurement techniques and effects on in-plane permeability of woven cloths in resin transfer moulding. Composites Part A: Applied Science and Manufacturing, **27**, 401–408 (1996). DOI: 10.1016/1359-835X(95)00028-Z

[14] Lundström T. S., Gebart B. R., Sandlund E.: In-plane permeability measurements on fiber reinforcements by the multi-cavity parallel flow technique. Polymer Composites, **20**, 146–154 (1999). DOI: 10.1002/pc.10342

[15] Demaría C., Ruiz E., Trochu F.: In-plane anisotropic permeability characterization of deformed woven fabrics by unidirectional injection. Part I: Experimental results. Polymer Composites, **28**, 797–811 (2007). DOI: 10.1002/pc.20107

[16] Buntain M. J., Bickerton S.: Compression flow permeability measurement: A continuous technique. Composites Part A: Applied Science and Manufacturing, **34**, 445–457 (2003). DOI: 10.1016/S1359-835X(03)00090-3

[17] Drapier S., Pagot A., Vautrin A., Henrat P.: Influence of the stitching density on the transverse permeability of non-crimped new concept (NC2) multiaxial reinforcements: Measurements and predictions. Composites Science and Technology, **62**, 1979–1991 (2002). DOI: 10.1016/S0266-3538(02)00127-6

[18] Mehri D., Michaud V., Kämpfer L., Vuilliomenet P., Månson J-A. E.: Transverse permeability of chopped fibre bundle beds. Composites Part A: Applied Science and Manufacturing, **38**, 739–746 (2007). DOI: 10.1016/j.compositesa.2006.09.006

[19] Elbouazzaoui O., Drapier S., Henrat P.: An experimental assessment of the saturated transverse permeability of non-crimped new concept (NC2) multiaxial fabrics. Journal of Composite Materials, **39**, 1169–1193 (2005). DOI: 10.1177/0021998305048746

[20] Scholz S., Gillespie J. W., Heider D.: Measurement of transverse permeability using gaseous and liquid flow. Composites Part A: Applied Science and Manufacturing, **38**, 2034–2040 (2007). DOI: 10.1016/j.compositesa.2007.05.002

[21] Ouagne P., Bréard J.: Continuous transverse permeability of fibrous media. Composites Part A: Applied Science and Manufacturing, **41**, 22–28 (2010). DOI: 10.1016/j.compositesa.2009.07.008

[22] Han N. L., Suh S. S., Yang J-M., Hahn H. T.: Resin film infusion of stitched stiffened composite panels. Composites Part A: Applied Science and Manufacturing, **34**, 227–236 (2003).
DOI: 10.1016/S1359-835X(03)00002-2

[23] Mathuw R., Advani S. G., Heider D., Hoffmann C., Gillespie J. W., Fink B. K.: Flow front measurements and model validation in the vacuum assisted resin transfer molding process. Polymer Composites, **22**, 477–490 (2001).
DOI: 10.1002/pc.10553

[24] Loos A. C., Rattazzi D., Batra R. C.: A three-dimensional model of the resin film infusion process. Journal of Composite Materials, **36**, 1255–1273 (2002).
DOI: 10.1177/0021998302036010168

[25] Yenilmez B., Senan M., Murat Sozer E.: Variation of part thickness and compaction pressure in vacuum infusion process. Composites Science and Technology, **69**, 1710–1719 (2009).
DOI: 10.1016/j.compscitech.2008.05.009

[26] Correia N. C., Robitaille F., Long A. C., Rudd C. D., Šimáček P., Advani S. G.: Analysis of the vacuum infusion moulding process: I. Analytical formulation. Composites Part A: Applied Science and Manufacturing, **36**, 1645–1656 (2005).
DOI: 10.1016/j.compositesa.2005.03.019

[27] Li J., Zhang C., Liang R., Wang B., Walsh S.: Modeling and analysis of thickness gradient and variations in vacuum-assisted resin transfer molding process. Polymer Composites, **29**, 473–482 (2008).
DOI: 10.1002/pc.20439

[28] Govignon Q., Bickerton S., Kelly P. A.: Simulation of the reinforcement compaction and resin flow during the complete resin infusion process. Composites Part A: Applied Science and Manufacturing, **41**, 45–47 (2010).
DOI: 10.1016/j.compositesa.2009.07.007

[29] Antonucci V., Giordano M., Nicolais L.: Liquid moulding processes. in 'Handbook of polymer blends and composites' (eds.: Kulshreshtha A. K., Vasile C.) Vol 2, 53–83, Rapra, Shrewsbury (2002).

[30] Drapier S., Monatte J., Elbouazzaoui O., Henrat P.: Characterization of transient through-thickness permeabilities of non crimp new concept (*NC*2) multiaxial fabrics. Composites Part A: Applied Science and Manufacturing, **36**, 877–892 (2005).
DOI: 10.1016/j.compositesa.2005.01.002

[31] Antonucci V., Giordano M., Nicolais L., Calabrò A., Cusano A., Cutolo A., Inserra S.: Resin flow monitoring in resin film infusion process. Journal of Materials Processing Technology, **143–144**, 687–692 (2003).
DOI: 10.1016/S0924-0136(03)00338-8

[32] Ballata W. O., Walsh S. M., Advani S.: Determination of the transverse permeability of a fiber preform. Journal of Reinforced Plastics and Composites, **18**, 1450–1464 (1999).
DOI: 10.1177/073168449901801601

[33] Giordano M., Nicolais L., Calabrò A. M., Cantoni S., Cusano A., Breglio G., Cutolo A.: A fiber optic thermoset cure monitoring sensor. Polymer Composites, **21**, 523–530 (2000).
DOI: 10.1002/pc.10207

[34] Niggemann C., Song Y. S., Gillespie J. W., Heider D.: Experimental investigation of the controlled atmospheric pressure resin infusion (CAPRI) process. Journal of Composite Materials, **42**, 1049–1061 (2008).
DOI: 10.1177/0021998308090650